N−H···π Interactions in Indole···Benzene-h_6,d_6 and Indole···Benzene-h_6,d_6 Radical Cation Complexes. Mass Analyzed Threshold Ionization Experiments and Correlated ab Initio Quantum Chemical Calculations

Julian Braun,[†] Hans Jürgen Neusser,*[,†] and Pavel Hobza*[,‡]

Institut für Physikalische und Theoretische Chemie, Technische Universität München, Lichtenbergstrasse 4, D-85747 Garching, Germany, and J. Heyrovský Institute of Physical Chemistry, Academy of Sciences of the Czech Republic and Center for Complex Molecular Systems and Biomolecules, 182 23 Prague 8, Czech Republic

Received: October 16, 2002; In Final Form: March 3, 2003

Indole−benzene complexes in the neutral and cationic forms were investigated by resonance enhanced two-photon ionization (REMPI) and mass analyzed threshold ionization (MATI) experiments and nonempirical ab initio quantum chemical methods. The experiment yields vibrational frequencies of the ionized complex in its ionic ground state. In addition, by observing the breakdown of the MATI signal at the cluster ion mass for a certain internal energy and its simultaneous appearance at the fragment mass, the dissociation energy of the ionic complex is found with high precision. Using a thermochemical cycle from this and the also measured adiabatic ionization energies of indole−benzene and indole, the dissociation energy of the neutral complex is found. The data were recently presented for indole−benzene-h_6 and are shown for indole−benzene-d_6 for the first time in this work. Stacked and N−H···π H-bonded structures of the neutral dimer were optimized using the approximative resolution of identity MP2 (RI-MP2) method combined with extended basis. The RI-MP2 treatment showed the preferential stability of the stacked structure while the CCSD(T) calculations favor the N−H···π H-bonded structure. The final stabilization enthalpy estimate (5.3 kcal/mol) agreed nicely with the experimental value of 5.2 kcal/mol (1823 ± 15 cm^{-1}) and points clearly to a N−H···π bounded structure of the complex. In the case of a radical cation, the stacked structure was shown not to be stable and was converted during optimization to the N−H···π H-bonded structure. The final stabilization enthalpy estimate (12.8 kcal/mol) agreed reasonably well with the experimental value of 13.1 kcal/mol (4581 ± 10 cm^{-1}). The theoretical harmonic intermolecular stretch frequency obtained for the neutral and cationic complexes (78 and 105 cm^{-1}) agreed fairly well with the experimental values (70 and 95 cm^{-1}). A surprisingly large N−H···π stabilization energy calculated for the benzene···indole complex supports speculation about the role of these interactions in the biological environment. The excellent agreement of the experimental and theoretical binding energies gives for the first time direct evidence that the theoretical treatment used can yield stabilization energies (enthalpies) of large molecular clusters differing from the experimental values by less than 0.5 kcal/mol.

Introduction

The noncovalent intermolecular interactions between systems containing aromatic rings are of primary importance in such important phenomena as base−base interactions in DNA and RNA or the tertiary structure of proteins. Two different types of this interaction exist, either interaction via π-electron clouds of both subsystems or X−H···π interaction. The relative importance of both interaction types was for a long time not known, and light was shed on this crucial problem through the experimental[1−8] and theoretical [9−16a] study of the simplest prototypical case, the benzene dimer. On the basis of these results, the following general conclusions were formulated: (i) a face-to-face highly symmetrical configuration is not stable; (ii) the T-shaped structure corresponds to the global minimum; (iii) the parallel-displaced (PD) structure corresponds to the local minimum and is only slightly less stable than the global minimum. The validity of these conclusions was confirmed by analyzing the benzene crystal where only T-shaped and PD motifs were found. Interaction of phenyl rings plays, however, a much broader role and determines also the structure of selected amino acids. For example, the crystal structure of phenylalanine is basically determined by the C−H···π and π···π (in the PD orientation) interactions.[16b] T-shaped and PD motifs were also recently found in the X···Y (X = benzene, Y = naphthalene or anthracene) complexes.[16c] The structure-making ability of the C−H···π interactions is surprising in light of the relative weakness of the interaction. Analyzing existing experimental and theoretical data for the benzene dimer, it can be concluded that C−H···π interactions are slightly stronger than the π···π (in the PD orientation) ones and both are lying in the interval 2.0−2.5 kcal/mol. This is not too strong an interaction, and for example, the average H-bond of the X−H···Y type (where X and Y are electronegative elements) is about twice as strong (the OH···O H-bond in the water dimer is close to 5 kcal/mol). The structure-making ability of the X−H···π contacts can be

* Corresponding authors. E-mail addresses: hobza@indy.jh-inst.cas.cz; neusser@ch.tum.de.

[†] Technische Universität München.

[‡] Academy of Sciences of the Czech Republic and Center for Complex Molecular Systems and Biomolecules.

10.1021/jp027217v CCC: $25.00
Published on Web 04/11/2003

magnified by increasing the polarity of the X−H bond, that is, by passing from a rather nonpolar C−H bond to much more polar N−H and O−H bonds. To obtain reliable estimates of these interactions, ab initio calculations should be performed with extended basis sets and cannot be limited to the low correlated level (e.g., MP2 one). Recently, several studies appeared[17−21] where X−H···π and π···π stabilization energies of the model systems were investigated; the total stabilization energy was constructed as a sum of the complete basis set limit of the MP2 stabilization energy and a correction term covering the higher correlation energy contributions. The N−H···π contacts were studied recently theoretically in the indole dimer[22] and pyrrole dimer.[23] The N−H···π H-bond found in the former complex (2.2 kcal/mol) was only slightly stronger than that in the benzene dimer while that in the latter complex was considerably stronger (5.1 kcal/mol). The N−H···π contacts were found in various crystals,[24−27] and their importance in the biological environment was discussed.

The aim of the present communication is to investigate experimentally (MATI spectroscopy) and theoretically (high-level ab initio quantum chemical calculations) complexes between indole and benzene in neutral as well as ionic states. There is a good reason for the combination of experiments and ab initio calculations. The present experiments provide accurate values for the stabilization enthalpies but do not provide rotational resolution and thus do not yield any direct information on the structure of the complex. On the other hand, the present experiment provides us with energetic and spectroscopic information not only of the neutral but also of the ionic system.

Experimental methods for direct determination of the structure of clusters are based on rotationally resolved spectroscopy. Microwave and infrared spectroscopy have provided valuable information on clusters, but these techniques hitherto have been restricted to clusters of small molecules. High-resolution rotationally resolved UV spectroscopy often can provide us with the information needed for structure determination. It has been successfully applied, for example, to the indole−water complex.[28,29] However, the indole−benzene dimer investigated in this work is too large for rotationally resolved spectroscopy. In principle, rotational coherence spectroscopy is a useful technique for larger systems but has not yet been applied to indole−benzene.[30] It remains to be seen whether the accuracy of the rotational constants achievable with this method is sufficient for a clear identification of the structure. For these reasons in the present work the experimental results for the binding energies and intermolecular frequencies of the indole−benzene dimer are compared with theoretical results for the structures and their respective binding energies. In this way from the measured binding energies information on the respective structures is obtained by comparison with theoretical results.

Several experimental techniques have been used for the measurement of cluster binding energies: Among them are mass spectrometric techniques,[31] infrared spectroscopy,[32] and IR spectroscopy combined with bolometric detection techniques.[33] Here we use the mass analyzed threshold ionization (MATI) method. After production of threshold ions with defined but variable internal energy, the dissociation threshold of the cluster ion is found by the appearance energy of the fragment daughter ions. From this value and the measured ionization energy, the dissociation threshold of the neutral cluster is deduced. For clusters the dissociation rate at threshold is expected to be high because of the small phase space of the intermolecular modes. Therefore, a kinetic shift of the dissociation threshold can be neglected and the measured thresholds are very close to the dissociation energies. No metastable mass peaks are detected in the mass spectrum on indole−benzene.

The problem of calculating the structure of indole−benzene is not trivial, and two entirely different structural types should be taken into consideration: N−H···π T-shaped and stacked ones. The first structure is characterized by a directed H-bond exhibiting typical features such as a red shift of the N−H stretch frequency and the intensity increase of this vibration band. The second structure is a typical noncovalent structure stabilized mainly by the London dispersion energy. While the theoretical treatment of the former systems is straightforward and satisfactory characteristics are mostly obtained already at the MP2 correlated level with medium basis sets, theoretical description of the latter systems requires a much higher theoretical level.[34] Here higher correlation contributions play a role and use of a method like the CCSD(T) method is required.[34]

The main problem represents, however, determination of the structure, and comparable results for both structural types can only be obtained if the MP2 method is combined with at least an extended basis set containing diffuse as well as polarization functions. In the case of DNA base pairs, we demonstrated[35] that the MP2/6-31G* treatment is not adequate (mainly for description of stacking interactions) and we extensively used the MP2/6-31G*(0.25) calculations. The main difference in both methods concerns the use of diffuse d-polarization functions. Instead of the standardly used exponent 0.8, we used the recommended[36] value 0.25. The method yields[35] surprisingly good stabilization energies, but it is impractical for the geometry optimization. The first level yielding acceptable geometries and stabilization energies of stacked and H-bonded structures is the MP2/aug-cc-pVDZ one. However, up to now it was not clearly shown whether higher-order correlation contributions do not change the stability order between H-bonded and stacked structures. Further, the basis set used ([4s3p2d/3s2p]) contains diffuse s-, p-, and d-functions required for proper description of dispersion energy. However, this basis set is unbalanced and, therefore, the use of (at least) a cc-pVTZ basis set ([4s3p2d1f/3s2p1d]) is recommended. It is evident that the MP2/cc-pVTZ optimization is not practical for extended complexes having more than 24 atoms (the benzene dimer with 24 atoms represents the boundary between medium and extended clusters). Recently, we explored[37] the applicability of the approximative resolution of the identity MP2 (RI-MP2) method[38−40] and have shown that the method combined with extended basis sets containing f-functions is capable of accurate description of H-bonded and stacked DNA base interactions. The results obtained[37] with the RI-MP2 method differ only marginally from those evaluated with the exact MP2 method, while the time saving is as larger as 1 order of magnitude. Let us mention at the end of this paragraph that the relative stability and relative importance of H-bonded and stacked structures represent one of the fundamental problems of today's science and, for example, the structure and function of DNA, RNA, and other nucleic acid architectures depend on the balance between planar H-bonding and stacking interaction of nucleic acid bases.

Methods

Experimental Method. The technique used in this work for measurement of binding energies is mass analyzed threshold ionization (MATI).[41,42] It has been described in detail in our recent work.[43] Briefly, MATI spectroscopy is based on the excitation of high ($n > 100$) long-lived Rydberg states and their subsequent ionization in a delayed pulsed electric field, leading to threshold ions in well-defined energy states. The simulta-

neously produced nonenergy-selected (prompt) ions are separated from the Rydberg states in a weak electric field of 0.6 V/cm in the present experiments. The Rydberg state series are converging to the various (vibrational) states of the cation, and the excited high Rydberg states are very close ($\sim$10 cm^{-1}) to the respective ionization energies. For an exciting laser light of approximately 0.3 cm^{-1} bandwidth and the separation field of 0.6 V/cm, the threshold ion peaks resulting from the pulsed field ionization of the high Rydberg states indicate the energetic position of the vibrational states of the cation within $\pm$5 cm^{-1} precision. Similar to zero-kinetic-energy (ZEKE) spectroscopy, MATI spectroscopy provides the vibrational spectrum of the ground electronic state of molecular or cluster cations. In addition, because of its mass selectivity the dissociation of cluster ions can be monitored by the MATI technique as a function of the selected internal energy of the ion. This is possible by the simultaneous monitoring of threshold ions at the cluster ion (parent) mass channel and the fragment (daughter) ion mass channel.[42,44] Applying a simple thermochemical cycle from the measured dissociation energy E_0 of the cluster ion and the measured adiabatic ionization energy (AIE) of the cluster and the aromatic molecule, the dissociation energy D_0 of the neutral cluster is found. In this way we have been able to find accurate values for the dissociation energy of several van der Waals complexes of polyatomic molecules with noble gases and for hydrogen-bonded aromatic molecule−water clusters.[45,46] In this work the MATI technique was used to measure the binding energy of the indole−C_6H_6 dimer in comparison with the one of indole−C_6D_6 and to compare these values with results from ab initio calculation. This allows us to draw conclusions about the character of the binding and the structure of the dimer.

Experimental Setup. The experimental setup used was described in detail elsewhere.[43] Briefly, it consists of two dye lasers pumped by an XeCl excimer laser yielding 10 ns light pulses with a bandwidth of 0.3 cm^{-1}. The two counterpropagating laser beams of different color intersect a skimmed supersonic molecular beam perpendicularly 15 cm downstream from the nozzle orifice. The light pulses overlap in space and time in the ion optics of a linear reflecting time-of-flight mass spectrometer.[47] The supersonic jet is obtained by expanding indole vapor which is produced inside a heated (110 °C) pulsed (25 Hz) valve and seeded in a mixture of Ne (3 bar) and 20 mbar benzene vapor into the vacuum. The excitation of indole clusters to high Rydberg states is achieved by a resonantly enhanced two-photon two-color process.The high Rydberg molecules are separated from the prompt ions by a weak electric field of 0.6 V/cm switched on about 100 ns after the occurrence of the two laser pulses in a first 30 mm wide zone of the ion optics.[48,49] Within several microseconds, the neutral high Rydberg molecules drift into a second 20 mm wide zone where no electric field is present at that time. A strong electric field of 500 V/cm is switched on 28 μs after the two laser pulses and ionizes the high Rydberg molecules. The resulting threshold ions are accelerated toward the ion reflector by this electric field and reflected toward the multichannel plates. Threshold spectra are recorded for ions of different mass selectively with a gated integrator/microcomputer system.

Quantum Chemical Calculations. *Neutral Dimer.* The geometries and interaction energies of both structures of the dimer were evaluated with the RI-MP2 method using the TZVPP basis set ([5s3p2d1f/3s2p1d]). Interaction energies were systematically corrected for the basis set superposition error (BSSE).[50] All the calculations were carried out using the TURBOMOLE 5.3 program suite,[51] and standard (default) auxiliary basis sets were adopted. For the geometries found, the stabilization energy was further evaluated with the same method but with a larger basis set (augTZVPP), obtained by addition of one set of diffuse s-, p-, d-, and f-functions.[52] The augTZVPP basis set was combined with the same auxiliary basis set as in the case of the TZVPP basis. For the sake of estimation of the complete basis set (CBS) limit of the RI-MP2 method, we used energies obtained with the mentioned augTZVPP basis and with the smaller augSVP basis set. The augSVP basis set was constructed by adding diffuse s-, p-, and d-functions[52] to the SVP basis set ([3s2p1d/2s1p]), and also here the auxiliary basis set optimized for the SVP basis set was adopted.

The CBS limit of the RI-MP2 interaction energies was estimated using simple extrapolation of interaction energy versus $1/N$, where N is the number of contracted AOs. We have shown recently[53] that this procedure gives very similar results as the more elaborated extrapolation technique suggested by Truhlar.[54]

The zero-point vibration energy (ZPVE) was determined at the MP2/6-31G* level, and all vibration frequencies were scaled by the recommended factor (0.943).[55]

The corrections to the higher-order correlation contributions (the difference between MP2 and CCSD(T) stabilization energies) were estimated for the RI-MP2/TZVPP geometries by performing the CCSD(T) single-point calculations utilizing the 6-31G**(0.25,0.15) basis set. We have shown recently[53] that the [MP2-CCSD(T)] correction term determined with the 6-31G**(0.25,0.15) basis set is close to the value found by using larger basis sets. It is important to mention that this concerns both planar H-bonded and stacked structures of the dimer.

The final stabilization energy (ΔE) was determined as follows:

$$\Delta E = \Delta E(\text{RI-MP2/CBS}) + \Delta\text{ZPVE}(\text{MP2/6-31G*}) + \Delta(\Delta E^{\text{MP2}} - \Delta E^{\text{CCSD(T)}})/\text{6-31G**(0.25,0.15)} \quad (1)$$

Radical Cation System. All the calculations for the open-shell systems were complicated due to slow convergence, and frequently the SCF and optimization procedures diverged. However, because the present system is charged, the lower-level calculations are expected to give reliable results. Specifically, already the unrestricted Hartree−Fock (UHF) calculations with the 6-31G* basis set give satisfactory geometry and stabilization energy. To estimate the role of correlation energy, we performed optimizations also with the unrestricted MP2 method (UMP2) using the same basis set as well as the larger aug-cc-pVDZ one. The ZPVE was determined at the UMP2/6-31G* level, and the corrections to the higher-order correlation contributions ($\Delta(\Delta E^{\text{MP2}} - \Delta E^{\text{CCSD(T)}})$ term) were estimated by performing the UCCSD(T) and UMP2 single-point calculations with the 6-31G basis set.

The final stabilization energy (ΔE) was determined as follows:

$$\Delta E = \Delta E(\text{MP2/aug-cc-pVDZ}) + \Delta\text{ZPVE}(\text{UMP2/6-31G*}) + \Delta(\Delta E^{\text{MP2}} - \Delta E^{\text{CCSD(T)}})/\text{6-31G} \quad (2)$$

Results and Discussion

Mass Analyzed Threshold Ionization Spectra. Using the MATI technique described above, threshold ion spectra of indole and indole−benzene clusters were recorded. For that, the first laser frequency was fixed to the $S_1(^1L_b) \leftarrow S_0,0^0_0$ transition of the respective cluster (35 067 cm^{-1} for indole−benzene-h_6 and indole−benzene-d_6). The second laser frequency was scanned

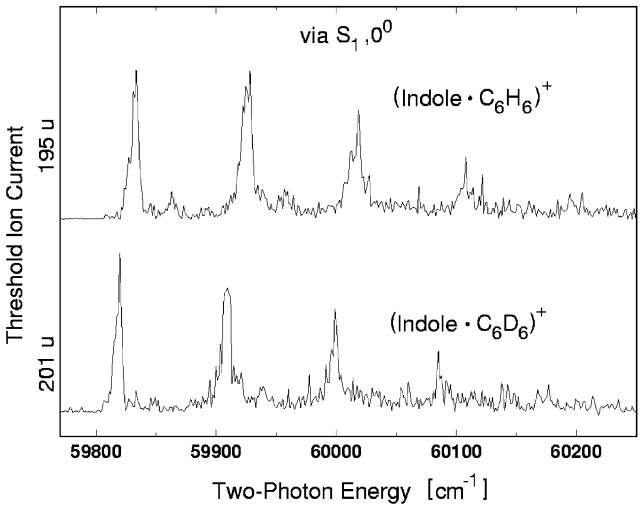

Figure 1. Threshold ion spectra of indole−benzene-h_6 (top trace) and indole−benzene-d_6 (bottom trace) in the vicinity of the adiabatic ionization energy given by the first peak in each spectrum. The peak series indicates a progression of an intermolecular vibration. For explanation, see text.

over the range of the high Rydberg states of the various ionization thresholds and threshold ions measured as a function of the second laser frequency with the technique described above.

In Figure 1 the result is shown for the region of the adiabatic ionization energy (AIE). In the upper trace the threshold ion spectrum of indole−benzene-h_6 is shown; in the lower trace is the respective result for indole−benzene-d_6. The first peak in the spectrum corresponds to the AIE and is located at 59 833 ± 5 cm^{-1} (59 819 cm^{-1}) in indole−benzene-h_6 (indole−benzene-d_6). It is shifted by 2785 cm^{-1} (2799 cm^{-1}) to the red of the bare indole. The dominating feature in the threshold ion spectrum is a 95 cm^{-1} (92 cm^{-1}) vibration forming a long progression. The slightly smaller frequency of the indole−benzene-d_6 complex is clearly seen for the higher (2nd and 3rd) progression members. We obtained similar results with long progressions also for the indole−H_2O clusters with a vibrational frequency of 189 cm^{-1} assigned as a stretching frequency of the intermolecular hydrogen bond.[56] The frequency observed for indole−benzene-h_6 is about half of the frequency of the stretching vibration in indole−H_2O. This is what we expect for an intermolecular vibration with stretching character in a hydrogen bond when taking into account the higher mass of the benzene moiety. A direct comparison of the experimental intermolecular frequency in the indole−benzene cation is performed with the theoretical results of this work. Unfortunately, long progressions of the corresponding intermolecular frequency in the neutral indole−benzene complex could not be observed in the intermediate spectrum because of small Franck−Condon factors. However, we found an additional peak at 69.5 cm^{-1} to the blue of the S_1,0° origin of indole−benzene-h_6. [56] It is interesting to compare this result with the calculated intermolecular vibrational frequencies presented in the next section.

In Figure 2 the measured threshold ion current is shown for higher two-photon energies. In this region the threshold ions are produced with internal energies in excess of 3000 cm^{-1}. In the upper (lower) two traces, the MATI spectra of indole−benzene-h_6 (-d_6) are shown measured at the parent mass 195 u (201 u) and the fragment (indole) ion mass 117 u. The parent ion signal breaks down at 64 414 cm^{-1} (64 455 cm^{-1}). No signal is observed on the fragment trace for low excitation energies,

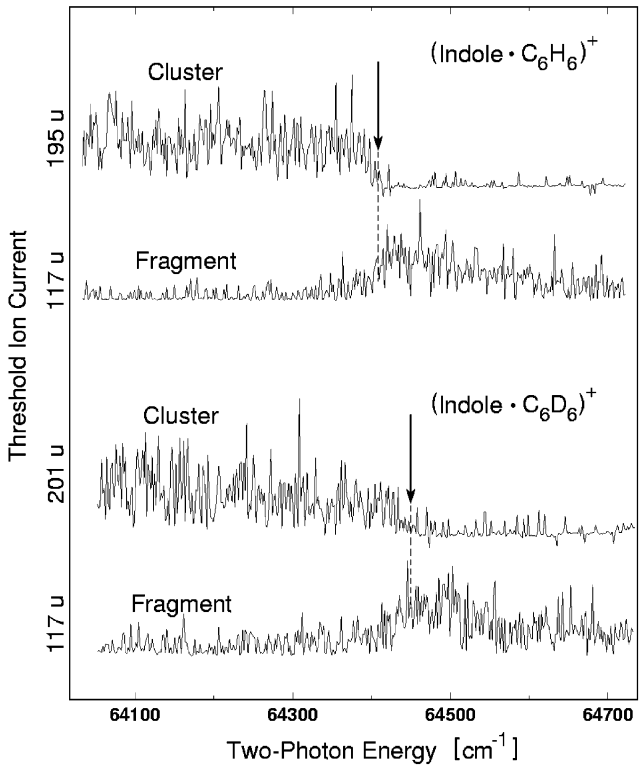

Figure 2. Threshold ion spectra of indole−benzene-h_6 (upper two traces) and indole−benzene-d_6 (lower two traces) measured at more than 4000 cm^{-1} above the adiabatic ionization energy. In each set of spectra the upper traces represent the threshold ion signal measured at the parent mass and the lower traces the threshold ion signal measured at the fragment mass. Note the slight blue shift of the breakdown of the parent ion signal in indole−benzene-d_6. For explanation of the arrows and discussion, see text.

but at roughly the same energy of the breakdown of the parent ion signal for each cluster, an onset of the fragment ion signal is observed. The ion signal rises or decreases within 20−40 cm^{-1}. If we take the 10% level of the parent signal as the dissociation threshold,[57] we find a clear blue shift of the dissociation threshold in indole−benzene-d_6 compared to the one of indole−benzene-h_6. From this result it is clear that, for the two-photon energy of 64 414 cm^{-1} (64 455 cm^{-1}) corresponding to an ion internal energy of 4581 cm^{-1} (4636 cm^{-1}), dissociation of the indole−benzene-h_6 (d_6) dimer takes place, resulting in an indole fragment ion. Taking into account the AIE of 59 833 cm^{-1} (59 819 cm^{-1}) of indole−benzene-h_6 (d_6), we find a dissociation energy E_0 of the ionic dimer of 4581 ± 10 cm^{-1} (4636 cm^{-1}). From a thermochemical cycle, we calculate $D_0 = E_0 - (AIE_{indole} - AIE_{indole-benzene})$, yielding $D_0 = 1823 \pm 15$ cm^{-1} (1864 cm^{-1}). The neutral indole−benzene binding energy is larger by more than a factor of 2 than the binding energies of mixed and homogeneous dimeric complexes of aromatic molecules such as benzene, *p*-difluorobenzene, and toluene found by various experimental methods.[47,58−62] Even if one takes into account that indole is larger than any of the molecules mentioned above, the factor of 2 larger binding energy points to a different type of binding in the indole−benzene dimer, that is, a π-hydrogen bonding.[56]

Correlated ab Initio Calculations. *Neutral System*. The optimized stacked and N−H···π H-bonded structures of the dimer are shown in Figure 3, and their characteristics are collected in Table 1. Contrary to expectation, the RI-MP2/TZVPP stabilization energy of the stacked structure is larger than that of the N−H···π H-bonded one. Including the zero-point energies, the difference becomes even larger and is close

TABLE 1. Energy Characteristics (in kcal/mol) for Various Structures of the Indole−Benzene Complex

structure[a]	ΔE RI-MP2/ TZVPP	ΔZPVE MP2/6-31G*	ΔE(MP2-CCSD(T)) 6-31G**(0.25, 0.15)	$\Delta H°$ [b]	$\Delta H°$ [c]
stacked	−6.571	0.118	−3.643	−2.810	
N−H$\cdots\pi$	−6.205[d,e]	0.635	−1.333	−4.237	−5.3

[a] Cf. Figure 1. [b] Interaction enthalpy at 0 K obtained as the sum of the ΔE, ΔZPVE, and ΔE(RI-MP2-CCSD(T)) terms. [c] Interaction enthalpy at 0 K obtained as the sum of the complete basis set limit of the RI-MP2 method and the ΔZPVE and ΔE(RI-MP2-CCSD(T)) terms. The experimental interaction enthalpy amounts to 1823 ± 15 cm^{-1} (5.2 kcal/mol). [d] The RI-MP2 interaction energies evaluated with the augSVP and augTZVPP basis sets for the RI-MP2/TZVPP geometry amount to −5.526 and −6.709 kcal/mol, respectively. [e] The complete basis set limit of the RI-MP2 method found by 1/N extrapolation from the augSVP and augTZVPP values amounts to −7.2 kcal/mol.

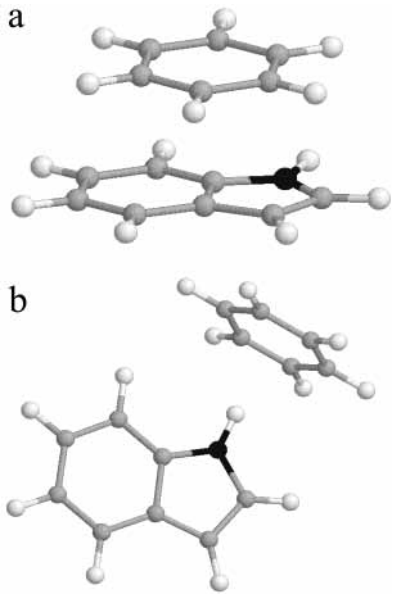

Figure 3. Optimized N−H$\cdots\pi$ H-bonded and stacked structures of indole$\cdots$benzene.

to 1 kcal/mol. The basis set used is large, and it is thus clear that the MP2 calculations will definitively prefer the stacked structure over the N−H$\cdots\pi$ H-bonded one. The MP2 treatment is, however, not sufficient and a higher-order correlation energy contribution should be considered. The CCSD(T) calculations performed with the 6-31G**(0.25,0.15) basis set changed the stability order dramatically. The [MP2-CCSD(T)] stabilization energy difference is for a stacked structure much larger (by more than 2 kcal/mol) than that for the N−H$\cdots\pi$ structure and leads to preferential stabilization of the H-bonded structure. The stabilization enthalpy of the N−H$\cdots\pi$ structure is now about 1.4 kcal/mol larger and supports the existence of an N−H$\cdots\pi$ H-bonded structure.

The indole N−H bond in the H-bonded structure is directed to the center of the benzene molecule (cf. Figure 3), and the distances of H and N (from the N−H bond of indole) to the benzene center of mass are 2.153 and 3.160 Å, respectively. The N−H$\cdots\pi$ structure is characterized by elongation of the N−H bond upon formation of the H-bond. This value depends on the theoretical level used, and the following results were found at the MP2/6-31G*, MP2/6-31G**, RI-MP2/augSVP, and RI-MP2/TZVPP levels: 0.0008, 0.0011, 0.0002, and 0.0030 Å. The largest elongation thus resulted from the most reliable RI-MP2/TZVPP calculations. For the sake of comparison, we present the elongation of the O−H bond in the water upon dimerization, calculated at the same theoretical level: 0.0070 Å.

To obtain the absolute value of the stabilization energy for the N−H$\cdots\pi$ H-bonded structure, it is necessary to consider the CBS limits of the RI-MP2 energy and correction to higher-order correlation contributions. The CBS limit of the RI-MP2 energy was obtained from augTZVPP and augSVP interaction energies (cf. Table 1). Addition of diffuse s-, p-, d-, and f-functions for non-hydrogen atoms and s-, p-, and d-functions for hydrogens to the TZVPP basis leads to a non-negligible stabilization energy increase (by 0.5 kcal/mol). It is to be mention that much more economical and faster augSVP calculations yield a very reasonable stabilization energy (5.526 kcal/mol). The CBS limit of the RI-MP2 stabilization energy (7.2 kcal/mol) is considerably larger than the TZVPP value and still larger than the augTZVPP value, which gives evidence about the necessity to consider the extrapolation to the CBS limit. On the other hand, the [MP2-CCSD(T)] correction term converges much faster to the CBS limit, and the present value obtained with the 6-31G**(0.25,0.15) basis set was shown[53] to be sufficiently close to the converged value. Summing the CBS limit of the RI-MP2 stabilization energy, the ΔZPVE, and the $\Delta(\Delta E^{MP2} - \Delta E^{CCSD(T)})$ correction term, we obtain the true stabilization enthalpy of 5.3 kcal/mol. This value nicely agrees with the experimental estimate of 5.2 kcal/mol (1823 cm^{-1}).

The vibration analysis of the N−H$\cdots\pi$ structure, performed at the MP2/6-31G* level, has shown that the structure does not correspond to the minimum because one vibration frequency with an imaginary value (−12 cm^{-1}) was found. Analyzing the respective mode, it appears that it corresponds to the rotation of the benzene around the intermolecular axis N−H$\cdots$center of mass of benzene. The five remaining intermolecular frequencies were localized at 8, 32, 71, 77, and 83 cm^{-1}, respectively, and the intermolecular stretch corresponds to the last one. After scaling by 0.943,[55] we obtained 78 cm^{-1}, and this value is in good agreement with the experimental result of 69.5 cm^{-1}. Also, the additional peak detected experimentally at 34.5 cm^{-1} agrees well with one of theoretical vibrations. Formation of the N−H$\cdots\pi$ structure is accompanying by the small red shift of the N−H stretch frequency. At the MP2/6-31G* level it is 7 cm^{-1}. Further, the calculated intensity of the respective band increased from 83 to 335 km/mol. Both these results support the classification of the N−H$\cdots\pi$ contact in the indole$\cdots$benzene complex as a weak H-bond. It is surprising, however, that such a strong complex (more than 5 kcal/mol) is characterized by such a small red shift. We are aware that a correlation between the red shift and the strength of the intermolecular interactions does not exist, but for complexes stronger than, for example, water dimer we expected a larger red shift.

The surprisingly large stabilization of the N−H$\cdots\pi$ structure of the indole$\cdots$benzene complex supports an idea about the structure-making ability of the aromatic N−H$\cdots\pi$ interactions. These interactions can exist in the nucleic acid complexes and also in amino acid complexes. The aromatic N−H bond exists in tryptophane and histidine and the aromatic ring in phenylalanine and thyrosine, and structures of all these complexes might be due to these interactions.

Radical Cation System. UHF/6-31G* gradient optimization

TABLE 2. Energy Characteristics (in kcal/mol) for the N−H···π H-bonded Structure of the Indole−Benzene Radical Cation

ΔE(MP2)[a]	ΔE(MP2)[b]	ΔZPVE (MP2)[a]	ΔE(MP2-CCSD(T))[c]	$\Delta H°$ [d]
−9.917	−12.322[e]	−0.599	0.142	-12.779

[a] 6-31G**. [b] aug-cc-pVDZ single point calculations performed for the MP2/6-31G** geometry. [c] 6-31G single point calculations performed for the MP2/6-31G** geometry. [d] Interaction enthalpy at 0 K obtained as the sum of the ΔE(MP2/aug-cc-pVDZ), ΔZPVE, and ΔE(MP2-CCSD(T)) terms. The experimental interaction enthalpy amounts to 4581 ± 10 cm^{-1} (13.1 kcal/mol).

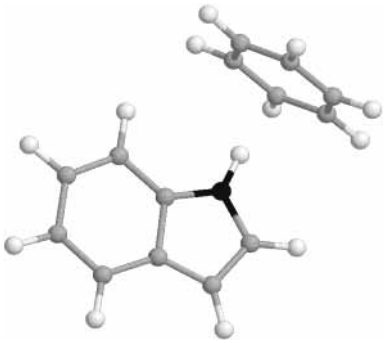

Figure 4. Optimized N−H···π H-bonded structure of the indole··· benzene radical cation.

was started for stacked and N−H···π structures, but both structures converged to the N−H···π H-bonded one which is visualized in Figure 4. The UMP2/6-31G* gradient optimization was thus performed only for this structure, and the energy characteristics are summarized in Table 2. Extension of the basis set from 6-31G* to aug-cc-pVDZ brings a significant increase of the stabilization energy. The ΔZPVE evaluated at the MP2/6-31G* level is very similar to that of the neutral system but is negative. The $\Delta(\Delta E^{MP2} - \Delta E^{CCSD(T)})$ correction term is small and positive, which means that the CCSD(T) stabilization energy is larger than the MP2 one. Putting all three contributions together, we obtain a true stabilization enthalpy of 12.8 kcal/mol, which is more than twice as large as that of the neutral system. Extension of the AO basis set yields enlargement of the stabilization enthalpy, and the present value thus represents the lower limit. We are aware of the fact that in the case of a radical cation the theoretical level is not as high as in the case of a neutral system. However, agreement with the experimental value (13.1 kcal/mol, 4581 cm^{-1}) is reasonable. Passing from indole−benzene-h_6 radical cation to indole−benzene-d_6 radical cation gives a decrease in the ΔZPVE(MP2) term from −0.599 to −0.683. The resulting ΔH term is thus changed from −12.8 kcal/mol (indole−benzene-h_6 radical cation) to −12.9 kcal/mol (indole−benzene-d_6 radical cation). This trend is well reproduced by experimental measurements where substitution of hydrogen by deuterium brings a dissociation energy increase of 55 cm^{-1} (0.16 kcal/mol).

The N−H bond of the indole radical cation is directed to the center of mass of benzene (similarly as in the case of a neutral system), and both subsystems in the radical cation are slightly closer. The distances of N and H atoms from the N−H bond of an indole radical cation from the benzene center of mass are 3.035 and 2.031 Å, respectively. Both distances are about 0.1 Å shorter than these distances in the neutral system. Similarly as in the neutral system, the N−H bond of the indole subsystem is elongated upon complex formation and the MP2/6-31G* value is 0.0034 Å, which is much more than that in the neutral system (0.0008 Å).

The vibration analysis performed at the MP2/6-31G* level indicated that the N−H stretch frequency is red shifted and the shift (37 cm^{-1}) is again larger than that in the neutral system. Because the intensity of the band increased (upon complex formation) from 357 to 947 km/mol, we can classify the complex as the H-bonded one. The intermolecular stretch frequency was found at 105 cm^{-1} (after scaling), and this value agrees again fairly well with the experimental value of 95 cm^{-1}.

Conclusions

1. Mass selected threshold ionization (MATI) experiments yield accurate values for the binding energy of neutral and ionized indole−benzene-h_6 (d_6) complexes but do not yield direct information on the structure of a complex. Structural information is obtained by performing the high-level correlated ab initio calculations.

2. Two energy minima were found at the potential energy surface of the indole−benzene complex. The MP2 calculations favor the stacked structure over the N−H···π H-bonded one. Passing, however, to the CCSD(T) level, the H-bonded structure becomes the global minimum.

3. The true stabilization enthalpy of the N−H···π H-bonded structure constructed as the CBS limit of the RI-MP2 stabilization energy, ΔZPVE, and the $\Delta(\Delta E^{MP2} - \Delta E^{CCSD(T)})$ correction term (5.3 kcal/mol) nicely agrees with the experimental value of 5.2 kcal/mol, which further supports the existence of this structural type.

4. In the case of the radical cation system, the stacked structure was not found and the global minimum corresponds again to the N−H···π H-bonded structure. The true stabilization enthalpy (12.8 kcal/mol) constructed similarly as in the case of the neutral system is considerably larger than that of the neutral system and agrees well with the experimental estimate (13.1 kcal/mol, 4581 cm^{-1}).

5. Intermolecular stretch frequencies of the neutral and cation systems calculated in both cases for the N−H···π H-bonded structures agree well with the experimental results.

6. Detailed experimental and theoretical investigation of the energetics of the N−H···π bonding for indole···benzene provides basic information for the intermolecular binding in biological systems, as the aromatic N−H···π motif is expected to play an important role in stabilizing structures of nucleic acids as well as amino acids.

Acknowledgment. This work was supported by a grant from the Grant Agency of the Academy of Sciences of the Czech Republic (A4040904). The authors thank the Deutsche Forschungsgemeinschaft and the Fonds der Chemischen Industrie for support of the experimental work.

References and Notes

(1) Janda, K. C.; Hemminger, J. C.; Winn, J. S.; Novick, S. E.; Harris, S. J.; Klemperer, W. *J. Chem. Phys.* **1975**, *63*, 1419.
(2) Börnsen, K. O.; Selzle, H. L.; Schlag, E. W. *J. Chem. Phys.* **1986**, *85*, 1726.
(3) Kiermeier, A.; Ernstberger, B.; Neusser, H. J.; Schlag, E. W. *J. Phys. Chem.* **1988**, *92*, 3785.
(4) Krause, H.; Ernstberger, B.; Neusser, H. J. *Chem. Phys. Lett.* **1991**, *184*, 411.
(5) Henson, B. F.; Hartland, G. V.; Venturo, V. A.; Felker, P. M. *J. Chem. Phys.* **1992**, *97*, 2189.
(6) Ebata, T.; Hamakado, M.; Moriyama, Y.; Ito, M. *Chem. Phys. Lett.* **1992**, *199*, 33.
(7) Arunan, E.; Gutowsky, H. S. *J. Chem. Phys.* **1993**, *98*, 4294.
(8) Venturo, V. A.; Felker, P. M. *J. Chem. Phys.* **1993**, *98*, 748.

(9) Williams, D. E. *Acta Crystallgr., Sect. A* **1980**, *36*, 715.
(10) Schauer, M.; Bernstein, E. R. *J. Chem. Phys.* **1985**, *82*, 3722.
(11) Karlström, G.; Linse, P.; Wallqvist, A.; Jönsson, B. *J. Am. Chem. Soc*. **1983,** *105*, 3777.
(12) Hobza, P.; Selzle, H. L.; Schlag, E. W. *J. Am. Chem. Soc*. **1994**, *116*, 3500.
(13) Hobza, P.; Selzle, H. L.; Schlag, E. W. *Chem. Rev*. **1994**, *94*, 1767.
(14) Hobza, P.; Selzle, H. L.; Schlag, E. W. *J. Phys. Chem*. **1996**, *100*, 18790.
(15) Sun, S.; Bernstein, E. R. *J. Phys. Chem.* **1996**, *100*, 13348.
(16) (a) Špirko, V.; Engkvist, O.; Soldán, P.; Selzle, H. L.; Schlag, E. W.; Hobza, P. *J. Chem. Phys.* **1999**, *111*, 572. (b) Hunter, C. A.; Singh, J.; Thornton, J. M. *J. Mol. Biol.* **1991**, *218*, 837. (c) Lee, N. K.; Park, S.; Kim, S. K. *J. Chem. Phys*. **2002**, *116*, 7902, 7910.
(17) Leininger, M. L.; Nielsen, I. M. B.; Colvin, M. E.; Janssen, C. L. *J. Phys. Chem. A* **2002**, *106*, 3850−3854.
(18) Tsuzuki, S.; Uchimaru, T.; Mikami, M.; Tanabe, K. *J. Phys. Chem. A* **2002**, *106*, 3867−3872.
(19) Tsuzuki, S.; Honda, K.; Uchimaru, T.; Mikami, M.; Tanabe, K. *J. Phys. Chem. A* **1999**, *103*, 8265.
(20) Tsuzuki, S.; Honda, K.; Uchimaru, T.; Mikami, M.; Tanabe, K. *J. Am. Chem. Soc*. **2000**, *122*, 3746.
(21) Hobza, P.; Riehn, C.; Weichert, A.; Brutschy, B. *Chem. Phys*., **2002**, *283*, 331.
(22) Pejov, L. *Chem. Phys. Lett*. **2001**, *339*, 269.
(23) Park, H.; Lee, S. *Chem. Phys. Lett.* **1999**, *301*, 487.
(24) Addlagatta, A.; Krzywda, S.; Czapinska, H.; Otlewski, J.; Jaskolski, M. *Acta Crystallogr. D57*, 649.
(25) Ciunik, Z.; Desiraju, G. *Chem. Commun*. **2001**, 703.
(26) Steiner, T.; Koellner, G. *J. Mol. Biol*. **2001**, *305*, 535.
(27) Brandl, M.; Weiss, M. S.; Jabs, A.; Suhnel, J.; Hilgenfield, R. *J. Mol. Biol.* **2001**, *307*, 357.
(28) Helm, R. M.; Clara, M.; Grebner, Th. L.; Neusser, H. J. *J. Chem. Phys. A* **1998**, *102*, 3268.
(29) Korter, T. M.; Pratt, D. W.; Küpper, J. *J. Phys. Chem. A* **1998**, *102*, 7211.
(30) Felker, P. M. *J. Phys. Chem.* **1992**, *96*, 7844.
(31) (a) Kemper, P. R.; Weis, P.; Bowers, M. T. *Int. J. Mass Spectrom. Ion Processes* **1996**, *160*, 17. (b) Ho, Y.-P.; Yang, Y.-Ch., Klippenstein, S. J.; Dunbar, R. C. *J. Phys. Chem. A* **1997**, *101*, 3338. (c) Rodgers, M. T.; Armentrout, P. B. *J. Phys. Chem. A* **1999,** *103*, 4955.
(32) Hunnicutt, S. S.; Branch, T. M.; Everhart, J. B.; Dudis, D. S. *J. Phys. Chem.* **1996**, *100*, 2083.
(33) Oudejans, L.; Miller, R. E. *J. Phys. Chem. A* **1997**, *101*, 7582.
(34) Hobza, P.; Müller-Dethlefs, K. *Chem. Rev.* **2000**, *100*, 4253.
(35) Hobza, P.; Šponer, J. *Chem. Rev.* **1999**, *99*, 3247.
(36) Kroon-Betenburg, L. M. J.; van Duijneveldt, F. B. *J. Mol. Struct.* **1985**, *121*, 185.
(37) Jurečka, P.; Nachtigall, P.; Hobza, P. *Phys. Chem. Chem. Phys.* **2001**, *3*, 4578.
(38) Feyereisen, M.; Fitzgerald, G.; Komornicki, A. *Chem. Phys. Lett*. **1993**, *208*, 359.
(39) Vahtras, O.; Almlöf, J.; Feyereisen, M. *Chem. Phys. Lett*. **1993**, *213*, 514.
(40) Bernholdt, D. E.; Harrison, R. J. *Chem. Phys. Lett.* **1996**, *250*, 470.
(41) Zhu, L: Johnson, P. M. *J. Chem. Phys*. **1991**, *94*, 5769.
(42) Krause, H.; Neusser, H. J. *J. Chem. Phys*. **1992**, *97*, 5923.
(43) Grebner, Th. L.; Neusser, H. J. *Chem. Phys. Lett.* **1995**, *245*, 578.
(44) Krause, H.; Neusser, H. J. *J. Chem. Phys*. **1993**, *99*, 6278.
(45) Grebner, Th. L.; Stumpf, R.; Neusser, H. J. *Int. J. Mass Spectrom. Ion Processes* **1997**, *167/168*, 649.
(46) For a review, see: Braun, J. E.; Mehnert, Th.; Neusser, H. J. *Int. J. Mass Spectrom. Ion Processes* **2000**, *203*, 1.
(47) Ernstberger, B.; Krause, H.; Kiermeier, A.; Neusser, H. J. *J. Chem. Phys*. **1990**, *92*, 5285.
(48) Merkt, F. *J. Phys. Chem.* **1994**, *100*, 2623.
(49) Dietrich, H. J.; Lindner, R.; Müller-Dethlefs, K. *J. Chem. Phys*. **1994**, *101*, 3399.
(50) Boys, S. F.; Bernardi, F. *Mol. Phys.* **1970**, *19*, 553.
(51) Ahlrichs, R.; Bär, M.; Häser, M.; Horn, H.; Kölmel, C. *Chem. Phys. Lett.* **1989**, *162*, 165.
(52) The exponents of the added diffuse functions were taken from Dunning's augmented correlation consistent polarized-valence basis sets (Dunning, T. H. J., Jr. *J. Chem. Phys*. **1993**, *98*, 1358).
(53) (a) Hobza, P.; Šponer, J. *J. Am. Chem. Soc*. **2002**, *124*, 11802. (b) Jurečka, P.; Hobza, P. *Chem. Phys. Lett*. **2002**, *365*, 89.
(54) Truhlar, D. G. *Chem. Phys. Lett.* **1998**, *294*, 45.
(55) Scheiner, S. *Hydrogen Bonding. A theoretical Perspective*; Oxford University Press: Oxford, U.K., 1997.
(56) Braun, J. E.; Grebner, Th. L.; Neusser, H. J. *J. Phys. Chem. A* **1998**, *102*, 3273.
(57) Grebner, Th. L.; von Unold, P.; Neusser, H. J. *J. Phys. Chem. A* **1997**, *101*, 158.
(58) Nishiyama, I.; Hanazaki, I. *Chem. Phys. Lett.* **1985**, *117*, 99.
(59) de Meijere, A.; Huisken, F. *J. Chem. Phys*. **1990**, *92*, 5826.
(60) Meot-Ner, M.; Hamlet. P.; Hunter, E. P.; Field, F. H. *J. Am. Chem. Soc*. **1978**, *100*, 5466.
(61) Kiermeier, A.; Ernstberger, B.; Neusser, H. J.; Schlag, E. W. *J. Phys. Chem.* **1988**, *92*, 3785.
(62) Ernstberger, B.; Krause, H.; Neusser, H. J. *Z. Phys. D* **1991**, *20*, 189.